

## CASE REPORT

# Clinical Imaging of Glycogen-rich Clear Cell Carcinoma of the Breast: A Case Series with Literature Review

Na Lae Eun<sup>1</sup>, Yoon Jin Cha<sup>2</sup>, Eun Ju Son<sup>1</sup>, Hye Mi Gweon<sup>1</sup>,  
Jeong-Ah Kim<sup>1</sup>, and Ji Hyun Youk<sup>1\*</sup>

Glycogen-rich clear cell carcinoma (GRCC) of the breast is a rare malignant tumor. Most previous reports focused on clinicopathologic findings of GRCC and imaging findings were not precisely described. Here, we report imaging findings of three cases of GRCC along with a literature review. GRCC of the breast was depicted as a mass with irregular or oval shape on mammography and complex cystic and solid composition or focal cystic change on ultrasound. GRCC showed internal high signal intensity on T<sub>2</sub>-weighted MRI with rim enhancement after contrast injection. These might suggest the possibility of GRCC in differentiating breast tumors.

**Keywords:** breast, glycogen-rich clear cell carcinoma, magnetic resonance imaging, ultrasound, mammography

## Introduction

Glycogen-rich clear cell carcinoma (GRCC) is a rare malignant breast tumor, which accounts for 0.9–3% of all breast carcinomas. This is histologically defined as a breast carcinoma in which more than 90% of tumor cells exhibit abundant clear cell cytoplasm containing glycogen.<sup>1</sup> To date, several previous studies for this rare disease entity have focused on clinicopathologic characteristics.<sup>2–11</sup> However, its imaging findings encompassing mammography, ultrasound, and MRI were not precisely described. Although imaging features from three different imaging modalities for GRCC were reported collectively in two cases,<sup>8,11</sup> detailed imaging features based on Breast Imaging Reporting and Data System (BI-RADS) lexicon have not been reported. Thus, we report three cases of GRCC in a radiologic perspective with imaging findings of mammography, ultrasound, and MRI along with a literature review.

## MRI Protocol

MR images were obtained using 1.5T system (Magnetom Avanto; Siemens, Erlangen, Germany) and 3T system

(Achieva; Philips Medical Systems, Best, the Netherlands) using a dedicated breast coil (Achieva; Philips Medical Systems). The patients routinely underwent turbo spin-echo T<sub>1</sub>- and T<sub>2</sub>-weighted sequences and a T<sub>2</sub>-weighted fat-suppressed spin-echo series. Dynamic contrast-enhanced MR study was performed with one pre-contrast and five post-contrast series using a fat-suppressed T<sub>1</sub>-weighted gradient echo sequence (1.5T system, TR/TE, 3.7/1.44; matrix 425 × 512; flip angle, 12°; FOV, 33 × 33 cm; sliced thickness, 1.5 mm and 3T system, TR/TE, 4.9/2.4; matrix, 340 × 340; flip angle, 12°; FOV, 34 × 34 cm; sliced thickness, 1.5 mm). Gadopentetate dimeglumine (Bono-I; Central Medical Service, Seoul, South Korea) or Gadobutrol (Gadovist, Bayer Healthcare, Berlin, Germany) was injected (0.1 mmol/kg body weight) using an automated injector (Nemoto; Nemoto Kyorindo, Tokyo, Japan) at a rate of 2 mL/sec, followed by a 20 mL saline flush. All MR exams were performed after the diagnosis of breast cancer by core-needle biopsy. The time intervals between breast biopsy and MRI were 14 days in average (range, 13–16 days).

## Case Reports

### Case 1

A 57-year-old woman visited our institution with the complaint of a palpable mass in her right breast. According to her medical records, she was postmenopausal and did not have any family history of breast cancer or other malignancy.

Mammography revealed an irregular, spiculated, hyperdense mass in the right upper outer area without visible microcalcification (Fig. 1A). On ultrasound, a 3-cm sized irregular, hypochoic mass was shown at the 11 o'clock direction of the right breast. The mass showed internal cystic

<sup>1</sup>Department of Radiology, Gangnam Severance Hospital, Yonsei University College of Medicine, 211 Eonju-ro, Gangnam-gu, Seoul 06273, Korea

<sup>2</sup>Department of Pathology, Gangnam Severance Hospital, Yonsei University College of Medicine, Seoul, Korea

\*Corresponding author, Phone: +82-2-2019-3510, Fax: +82-2-3462-5472, E-mail: jhyouk@yuhs.ac

©2018 Japanese Society for Magnetic Resonance in Medicine  
This work is licensed under a Creative Commons Attribution-NonCommercial-NoDerivatives International License.

Received: January 24, 2018 | Accepted: July 11, 2018

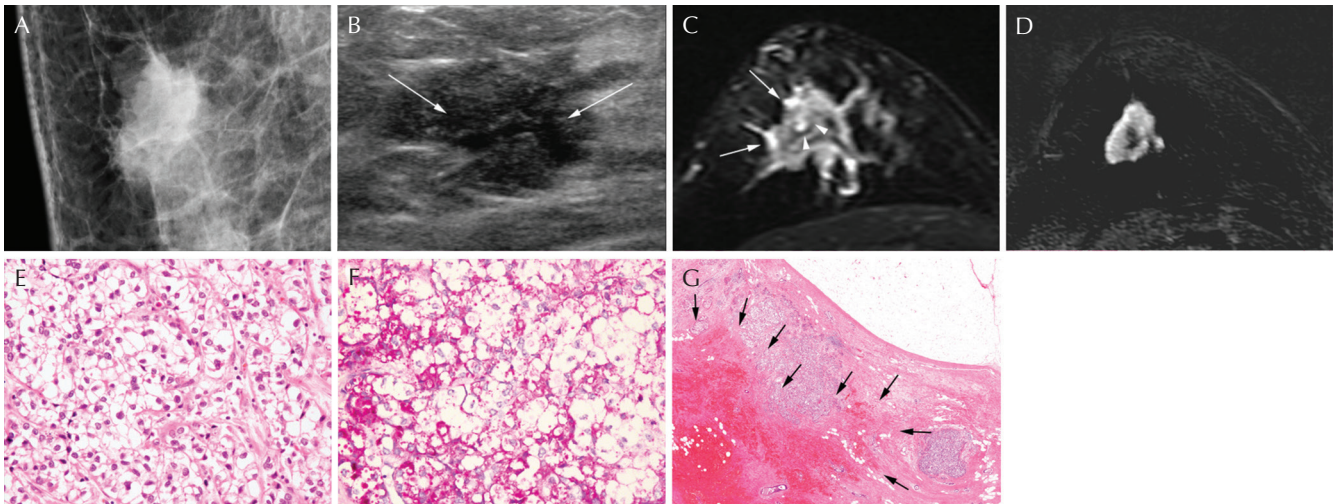


**Fig. 1** A 57-year-old woman with glycogen-rich clear cell carcinoma (GRCC) in the right breast. (A) Mediolateral oblique view of mammography shows an irregular, spiculated, and hyperdense mass in the upper central quadrant of the right breast. (B) Ultrasonography presents an irregular, spiculated, and hypoechoic mass with internal cystic change in the central portion (arrows). (C) On  $T_2$ -weighted MRI, the mass shows intermediate to low signal intensity with peritumoral edema (arrows) and internal high signal intensity (arrowheads), suggesting cystic portion. (D) The tumor is shown as an irregular, spiculated mass with rim enhancement on subtracted images after contrast injection. (E) The tumor cells show polygonal contour with clear cytoplasm and distinct cell membrane (Hematoxylin and eosin [H&E] stain  $\times 400$ ). (F) Intracytoplasmic glycogen is highlighted by Periodic acid-Schiff stain (PAS stain,  $\times 400$ ). (G) The tumor mass showed internal cystic portion and hemorrhage (arrows) (H&E stain,  $\times 17$ ).

change in the central portion (Fig. 1B). On MRI, an irregular, spiculated mass was observed in the right upper outer area, showing focal high signal intensity and peritumoral edema on  $T_2$ -weighted imaging (Fig. 1C). On dynamic contrast-enhanced  $T_1$ -weighted images with subtraction, the mass showed rim enhancement with fast enhancement and wash-out kinetics (Fig. 1D). The final BI-RADS assessment was category 5, highly suggestive of malignancy.

After mastectomy, the final pathologic diagnosis was GRCC. Microscopically, tumor cells showed moderate nuclear atypia, intracytoplasmic glycogen, and sharply-defined cell borders. Most of the tumor cells had clear cytoplasm and occasional intracytoplasmic glycogen as fine granular materials, which was Periodic acid-Schiff (PAS)-positive and diastase-labile (Fig. 1E and 1F). The tumor mass showed internal cystic portion and hemorrhage (Fig. 1G).

### Case 2

A 67-year-old woman presented with a palpable mass in her left breast. She had no family history of breast cancer and was postmenopausal status.

On mammography, an oval, indistinct, hyperdense mass without microcalcification was noted in the left upper outer area (Fig. 2A). At ultrasound, the mass showed oval shape, microlobulated margin, and hypoechogenicity with 2 cm in size at the left 1 o'clock direction (Fig. 2B). On color Doppler examination, several peripheral vessels were noted at the upper rim of the mass (Fig. 2C). Shear-wave elastography showed an irregular mass with red, heterogeneous color map pattern. The mean elasticity value of the mass was 176.8 kPa and the elasticity ratio of the mass to the reference fat tissue

was 16.4 measured by placing ROI over the stiffest part of the lesion and surrounding the fat tissue (Fig. 2D). MRI revealed an oval, irregular mass at the left upper portion of breast. The mass showed intermediate signal intensity with multiple internal hyperintense foci and peritumoral edema on  $T_2$ -weighted imaging (Fig. 2E). On dynamic contrast-enhanced  $T_1$ -weighted images with subtraction, the mass presented rim enhancement with fast enhancement and wash-out kinetics pattern (Fig. 2F). The final BI-RADS assessment was category 5, highly suggestive of malignancy.

After breast-conserving surgery, the final pathologic diagnosis was GRCC showing focal cystic portion.

### Case 3

A 49-year-old woman complained of a palpable mass in her left breast. She was premenopausal and had no family history of breast cancer or other malignancy.

Mammography showed an oval, circumscribed hyperdense mass in her upper breast without evidence of microcalcification (Fig. 3A). On ultrasound, an oval, complex cystic, and solid mass was presented at the left 12 o'clock direction with the size of 1.4 cm (Fig. 3B). The solid portion of the mass showed hypoechogenicity and circumscribed margin. At MRI, the mass demonstrated oval shape and circumscribed margin in the upper inner quadrant of the left breast. The solid portion of the mass showed intermediate signal intensity and the cystic portion of the mass showed high signal intensity on  $T_2$ -weighted imaging (Fig. 3C). On dynamic contrast-enhanced  $T_1$ -weighted images with subtraction, the mass exhibited an oval and circumscribed mass showing rim enhancement with fast enhancement and

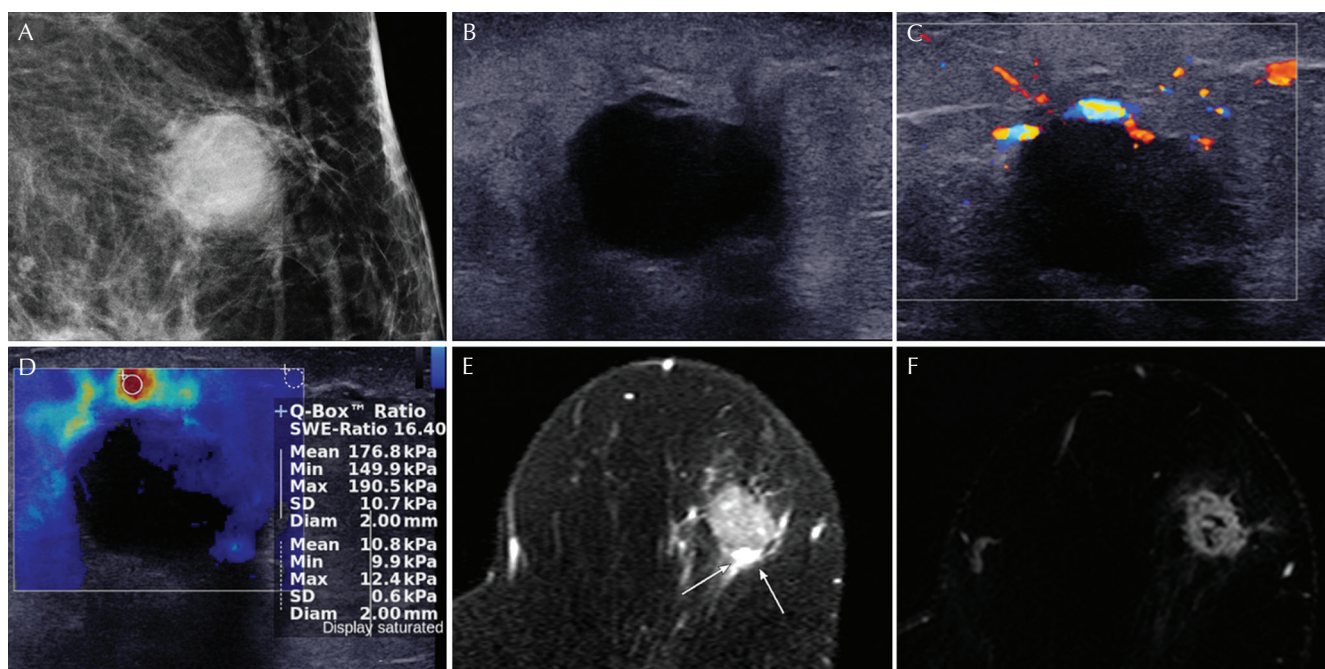


**Fig. 2** A 67-year-old woman with glycogen-rich clear cell carcinoma (GRCC) in the left breast. (A) Mediolateral oblique view of mammography shows an oval, indistinct, high density mass at the upper outer quadrant of the left breast. (B) On ultrasound, the mass shows hypoechogenicity and microlobulated margin. (C) Several peripheral vessels are seen at the upper rim on doppler examination. (D) On shear-wave elastography, the mass shows red, heterogeneous elasticity. The mean elasticity value of the mass was 176.8 kPa and the elasticity ratio of the mass to the reference fat tissue was 16.4 measured by placing ROI over the stiffest part of the lesion and surrounding fat tissue. (E) On T<sub>2</sub>-weighted MRI, the mass shows intermediate to high signal intensity with peritumoral edema in the posterior portion (arrows). (F) On dynamic contrast-enhanced images with subtraction, the mass shows oval shape, irregular margin and rim enhancement.

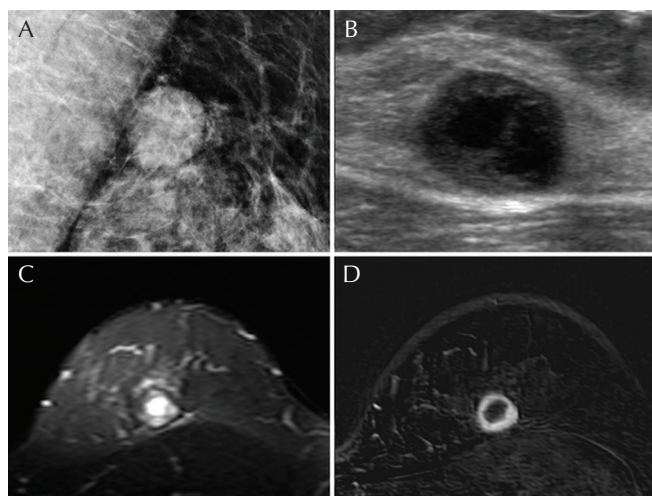


**Fig. 3** A 49-year-old woman with glycogen-rich clear cell carcinoma (GRCC) in the left breast. (A) Mediolateral oblique view of mammography shows an oval, circumscribed hyperdense mass at the upper central quadrant of the left breast. (B) Ultrasonography reveals a thick-walled complex cystic and solid mass with circumscribed margin. (C) On T<sub>2</sub>-weighted MRI, the solid portion of the mass shows intermediate signal intensity and the cystic portion at the center shows high signal intensity. (D) Dynamic contrast-enhanced image with subtraction shows an oval, circumscribed mass with rim enhancement.

wash-out kinetics (Fig. 3D). The final BI-RADS assessment was category 4B, moderate suspicion for malignancy.

The final pathologic diagnosis was GRCC after surgery. The internal cystic portion was also noted in the mass.

### Discussion

GRCC is a rare variant of breast carcinoma. The pathologic feature of GRCC is characterized by almost entirely of polygonal cells with clear cytoplasm containing PAS-positive, diastase-labile glycogen, which is extracted during processing for histological sections leaving vacuolated cytoplasm.<sup>1</sup> Differential diagnosis includes lipid-rich carcinoma, signet ring carcinoma, myoepithelial tumor, endocrine tumor, secretory variant ductal or lobular carcinoma, and sebaceous carcinoma.<sup>12</sup> GRCC also develops in organs other than breast, such as the lung, kidney, salivary gland, ovary, and endothelium.<sup>4</sup> This presents at a median age of 53 years and the prognosis is still controversial.<sup>9</sup> Regarding imaging findings of GRCC, most previous cases were reported sporadically (Table 1). Even in the largest study of 28 cases of GRCC, the information of imaging features was limited.<sup>9</sup> About 40% of mammographic and ultrasound features were missing and descriptors were not based on BI-RADS.

**Table 1** Publications regarding imaging findings of glycogen-rich clear cell carcinoma of the breast: revised according to BI-RADS

Author (year)	Number of cases	Mammography	Ultrasound	MRI
Baslaim et al. (2017) <sup>11</sup>	1	Irregular mass with microlobulated margin and microcalcifications	Irregular, hypoechoic mass with microlobulated margin with vessels in rim	Irregular mass with enhancement
Ratti et al. (2015) <sup>10</sup>	1	Round, hyperdense mass without microcalcification	Solid, heterogeneous echoic mass	NA
Ma et al. (2014) <sup>9</sup>	28	High-density mass with intratumoral calcifications	Hypoechoic mass with calcifications	NA
Salemis (2012) <sup>8</sup>	1	Isolated group of microcalcifications	Hypoechoic nodules with irregular margins and posterior acoustic enhancement	Multiple, irregular, rim enhancing lesions
Martín-Martín et al. (2011) <sup>7</sup>	1	Round, high-density mass with partially irregular margins and microcalcifications	Solid, heterogeneous mass	NA
Mizukami et al. (2009) <sup>6</sup>	1	Obscured by the dense breast tissue without microcalcifications	Irregular, hypoechoic mass with spiculated margin and posterior acoustic enhancement	NA
Markopoulos et al. (2008) <sup>5</sup>	1	Oval, microlobulated mass without microcalcifications	Solid, hypoechoic mass with circumscribed margin	NA
Pak et al. (2005) <sup>4</sup>	1	Irregular mass with spiculated margin without microcalcifications	NA	NA
Trupiano et al. (2003) <sup>3</sup>	1	Irregular, spiculated mass with areas of microcalcifications	NA	NA
Satoh et al. (1998) <sup>2</sup>	1	Irregular mass with spiculated margin and microcalcifications	Hypoechoic mass with spiculated margin and heterogeneous echogenicity	NA

BI-RADS, Breast Imaging Reporting and Data System; NA, not available.

In addition, elastographic ultrasound feature as a recently developed ultrasound technique has not been reported.

The most common mammographic finding of GRCC has been reported as an irregular mass with microcalcifications (Table 1).<sup>2,3,9,11</sup> In the previous study for 28 cases of GRCC, 33.3% was associated with calcifications visible on mammography.<sup>9</sup> In another case report, abundant calcifications and inflammatory infiltrates in the extensive necrotic portion of GRCC was pathologically observed.<sup>7</sup> Among 27 cases of GRCC available from previous reports (10 mammographic findings out of 28 cases of GRCC were lost in Ref. 9) (Table 1), 16 cases (59.3%) showed irregular mass and 14 cases (51.9%) presented microcalcifications on mammography. However, none of our cases showed microcalcifications visible on mammography and two masses of our series presented oval shape which were also shown in previous reports.<sup>5,7,10</sup> Thus, GRCC is regarded to demonstrate relatively variable features on mammography.

In literature, most ultrasound findings of GRCC were not characteristic, that is, a hypoechoic or heterogeneous mass with spiculated margin.<sup>2,6,8</sup> Some cases revealed microlobulated or even circumscribed margin.<sup>5,10,11</sup> In the previous

study including 28 cases of GRCC,<sup>9</sup> limited and nonspecific ultrasound features were described, such as hypoechoic masses with or without calcifications. Likewise, the sonographic shape or margin of GRCC was also various in our series. However, it was interesting that internal anechoic cystic component was demonstrated in two cases, which have not been reported as ultrasound findings of GRCC in literature. At shear-wave elastography, GRCC showed high mean elasticity value over 100 kPa enough to be diagnosed as malignancy and an irregular mass with red, heterogeneous elasticity by visual assessment.

On MRI, all GRCC in our series showed internal high signal intensity on T<sub>2</sub>-weighted imaging, suggesting internal cystic change. This was consistent with the ultrasound feature of internal anechoic cystic component as mentioned above. Internal cystic portion was also found on pathology of our cases. Similarly, several reports have demonstrated cystic changes of GRCC in other organs. Clear cell carcinoma of the kidney, which is composed of intraplasmic glycogen and lipid, was reported to have necrosis, hemorrhage or cysts on pathology and show cystic change on MR images, up to 15%.<sup>13</sup> Ovarian clear cell carcinoma also has been shown as

predominantly cystic mass or solid mass with cystic areas or necrosis on MRI.<sup>14</sup> These pathologic and imaging characteristics of clear cell carcinomas of the kidney and ovary were in accordance with imaging features of our cases of GRCC. Although observed in a few cases, therefore, the internal cystic change might be one of the characteristic imaging features of GRCC, considering the concordant ultrasound, MRI features and corresponding pathology.

In addition, peritumoral edema, which is defined as high signal intensity around or posterior to the mass in T<sub>2</sub>-weighted image, was observed in our two cases.<sup>15</sup> Although some features of changes after biopsy can be confused with peritumoral edema, these might not have influenced in our cases because there were intervals of 13–16 days between MR exams and core-needle biopsy. The mechanisms of peritumoral edema are not fully understood, but several reports have suggested that peritumoral edema may be caused by increased vascular permeability and peritumoral cytokines due to increased peritumoral pressure or newly developed tumor vessels.<sup>15</sup> In a previous study, this peripheral T<sub>2</sub> hyperintensity was observed in 20% of breast carcinoma, which was larger than 1 cm in size and it was significantly rim enhancement pattern.<sup>16</sup> For contrast-enhanced MRI, scarcely reported were the morphologic features of GRCC and no kinetic features in dynamic images have been reported (Table 1).<sup>8,11</sup> The morphologic feature was irregular enhancing masses in previous reports. In our series, all GRCC was depicted as enhancing masses with fast enhancement and wash-out kinetics, suggesting malignancy. In addition, all GRCC showed characteristically rim enhancement, which was also observed in one previous report.<sup>8</sup> Peritumoral edema and rim enhancement were reported to be associated with poor survival outcomes of invasive breast cancer.<sup>17</sup> Although there has been controversy over the prognosis of GRCC, several researchers have reported that the prognosis of GRCC is poorer with decreased survival than that of invasive ductal carcinoma.<sup>9</sup>

## Conclusion

GRCC showed complex cystic composition or focal cystic change at ultrasound. On MRI, GRCC showed internal high signal intensity on T<sub>2</sub>-weighted imaging and rim enhancement on contrast-enhanced imaging. These imaging findings might suggest the possibility of GRCC in differentiating breast tumors.

## Conflicts of Interest

The authors declare that they have no competing interests.

## References

- Toikkanen S, Joensuu H. Glycogen-rich clear-cell carcinoma of the breast: a clinicopathologic and flow cytometric study. *Hum Pathol* 1991; 22:81–83.
- Satoh F, Umemura S, Itoh H, et al. Fine needle aspiration cytology of glycogen-rich clear cell carcinoma of the breast. A case report. *Acta Cytol* 1998; 42:413–418.
- Trupiano JK, Ogradowczyk E, Bergman S. Pathologic quiz case: mass in the right breast. Glycogen-rich clear cell carcinoma of the breast. *Arch Pathol Lab Med* 2003; 127:1629–1630.
- Pak I, Kutun S, Celik A, Alyanak A, Ardic F, Cetin A. Glycogen-rich “clear cell” carcinoma of the breast. *Breast J* 2005; 11:288.
- Markopoulos C, Mantas D, Philipidis T, et al. Glycogen-rich clear cell carcinoma of the breast. *World J Surg Oncol* 2008; 6:44.
- Mizukami Y, Takayama T, Takemura A, Ichikawa K, Onoguchi M, Taniya T. Glycogen-rich clear cell carcinoma of the breast: a case report. *J Med Ultrason* (2001) 2009; 36:39–43.
- Martín-Martín B, Berná-Serna JD, Sánchez-Henarejos P, López-Poveda MJ, Berná-Mestre JD, Rodríguez-García JR. An unusual case of locally advanced glycogen-rich clear cell carcinoma of the breast. *Case Rep Oncol* 2011; 4:452–457.
- Salemis NS. Intraductal glycogen-rich clear cell carcinoma of the breast: a rare presentation and review of the literature. *Breast Care (Basel)* 2012; 7:319–321.
- Ma X, Han Y, Fan Y, Cao X, Wang X. Clinicopathologic characteristics and prognosis of glycogen-rich clear cell carcinoma of the breast. *Breast J* 2014; 20:166–173.
- Ratti V, Pagani O. Clear cell carcinoma of the breast: a rare breast cancer subtype - case report and literature review. *Case Rep Oncol* 2015; 8:472–477.
- Baslaim MM, Junainah EM, Ahmad HH, et al. Glycogen rich clear cell carcinoma (GRCC) of the breast may not have a poor prognosis. *Int J Surg Case Rep* 2017; 33: 92–96.
- Hayes MM, Seidman JD, Ashton MA. Glycogen-rich clear cell carcinoma of the breast. A clinicopathologic study of 21 cases. *Am J Surg Pathol* 1995; 19:904–911.
- Prasad SR, Humphrey PA, Catena JR, et al. Common and uncommon histologic subtypes of renal cell carcinoma: imaging spectrum with pathologic correlation. *Radiographics* 2006; 26:1795–1806; discussion 1806–1810.
- Wang W, Ding J, Zhu X, Li Y, Gu Y, Peng W. Magnetic resonance imaging characteristics of ovarian clear cell carcinoma. *PLoS One* 2015; 10:e0132406.
- Uematsu T. Focal breast edema associated with malignancy on T<sub>2</sub>-weighted images of breast MRI: peritumoral edema, prepectoral edema, and subcutaneous edema. *Breast Cancer* 2015; 22:66–70.
- Kawashima H, Kobayashi-Yoshida M, Matsui O, Zen Y, Suzuki M, Inokuchi M. Peripheral hyperintense pattern on T2-weighted magnetic resonance imaging (MRI) in breast carcinoma: correlation with early peripheral enhancement on dynamic MRI and histopathologic findings. *J Magn Reson Imaging* 2010; 32:1117–1123.
- Song SE, Shin SU, Moon HG, Ryu HS, Kim K, Moon WK. MR imaging features associated with distant metastasis-free survival of patients with invasive breast cancer: a case-control study. *Breast Cancer Res Treat* 2017; 162:559–569.